Monodisperse Chemically Modified Graphene Obtained by Density Gradient Ultracentrifugal Rate Separation

Xiaoming Sun,* Dachao Luo, Junfeng Liu, and David G. Evans

State Key Laboratory of Chemical Resource Engineering, Beijing University of Chemical Technology, P.O. Box 98, Beijing 100029, China

ABSTRACT A simple density gradient ultracentrifuge separation method has been developed for sorting chemically modified graphene (CMG) by sheet size and surface chemistry in just a few minutes. By optimizing the parameters, including the density gradient and centrifugation time, CMG sheets with specific size ranges and optical properties can be targeted selectively. UV—vis absorbance and photoluminescence spectra revealed the properties of separated CMG samples are highly dependent on their sheet size and degree of oxidation. A possible mechanism for the separation is discussed.

KEYWORDS: graphene · density gradient · separation · ultracentrifuge · monodisperse

Graphene is a one-atom-thick two-dimensional carbon system and has been suggested as a potential alternative to single walled carbon nanotubes and monocrystalline silicon for future technological applications in many fields such as nanoelectronics, sensors, nanocomposites, batteries, supercapacitors and hydrogen storage, due to its low cost and novel properties.[1−7] One of the prerequisites for exploiting these potential applications is the availability of bulk quantities of graphene sheets with appropriate sizes and specific functionalization. For instance, single-layered graphene sheets with lateral sizes of micrometers and limited surface functionalization are required for use in many devices,[8−12] while applications in cellular imaging and drug delivery require molecular sized graphene samples (typically <20 nm) with a fully functionalized surface in order to interface with biological systems.[13−15] In other cases, take electronic film preparation[16−19] for example, the size and surface chemistry of the graphene "building blocks" might influence the properties of the final products.

A variety of methods have been developed to prepare chemically modified graphene (CMG) with specific functionalization.[12,20−29] Those which involve the formation of a colloidal suspension of graphene oxide (GO) from graphite have attracted considerable attention due to their reliability, amenability to large-scale production, relatively low material cost, and versatility in terms of chemical functionalization. Although the process results in residual oxygen-containing functional groups on the sheets that lead to some loss in electron mobility, it offers much greater flexibility in terms of overall materials properties. However, it still remains a challenge to obtain monodisperse CMG sheets with precisely tailored size and surface chemistry in bulk quantities by synthesis optimization alone. The preparation of CMG commonly involves oxidation/exfoliation of graphite and subsequent chemical reduction.[5,30,31] The oxidation step is a random "top-down" chemical cutting process which does not allow precise control over size or shape and does not result in monodisperse samples of CMG, unlike the types of monodisperse inorganic nanoparticles which are routinely obtained by well controlled "bottom-up" syntheses.[32,33] At the same time, because the carbon atoms in the core of a graphite particle are less chemically accessible during oxidation than those at the surface/edges, the as-obtained graphene oxide particles usually have different degrees of oxidation, which might interfere with or complicate subsequent processing.

An efficient way to address this problem is by performing "post-synthesis" separation to sort graphene or CMG according to their differences in sheet size and surface chemistry. The isopycnic density gradient ultracentrifugation (DGU) separation method has been applied to separate carbon nanotubes by diameter/chirality/wall

*Address correspondence to sunxm@mail.buct.edu.cn

Received for review January 8, 2010 and accepted April 28, 2010.

Published online May 5, 2010.
10.1021/nn1000386

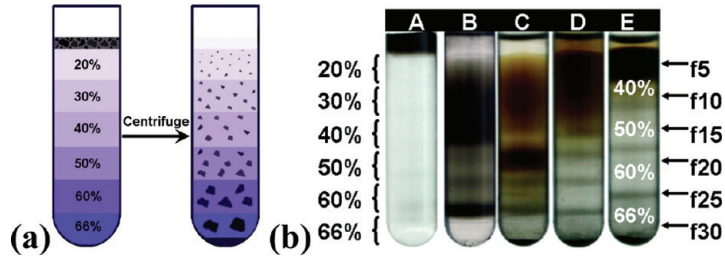

Figure 1. (a) Schematic illustration of the mechanism of DGUR separation of CMG sheets with different sizes. (b) Digital camera images of the ultracentrifuge tubes after separation at 50K rpm: (A) before separation; (B) CRG separated in a 20−66% gradient for 15 min; (C) GO separated in a 20−66% gradient for 15 min; (D) GO separated in a 20−66% gradient for 5 min; (E) GO separated in a 40−66% gradient for 5 min.

thickness[34−38] and separate graphene by number of layers.[39,40] These separations involve balancing the density of colloids of the material with that of a supporting medium.[35,36] Due to the high density of CMG, separation by isopycnic DGU is not possible (in contrast to surfactant encapsulated unmodified graphene[39,40]). Here we show how an alternative procedure—density gradient ultracentrifugal rate (DGUR) separation—which relies on the dependence of the sedimentation rate of colloidal nanoparticles on their size and geometry, may be utilized effectively to separate CMG samples. The DGUR method has previously been employed for separation of SWCNTs by length,[41,42] separation of colloidal metal nanoparticles by size,[43] and size-dependent separation of pegylated graphene oxide.[13] However, separation of bare single layers of CMG by size and chemical nature has not yet been reported. By optimizing the DGUR separation parameters, we can obtain CMG—that is, graphene oxide (GO) and chemically reduced graphene oxide (CRG)—sheets with a specific size range and with particular properties for different applications. This separation method is expected to be a general postprocessing approach with wide application in nanoscience and nanotechnology.

RESULTS AND DISCUSSION

The DGUR method, which takes advantage of the differences in sedimentation rate between various sized nanoparticles, has been adapted from biomacromolecule purification.[13,34,41,42,44] A schematic illustration of the DGUR separation system for CMG sheets is shown in Figure 1a. When a CMG suspension is placed on top of the multilayer step density gradient and centrifuged, the action of centripetal forces results in the CMG colloids being driven through the liquid gradient. Larger sheets have a higher sedimentation rate according to Stokes' Law[45] after balancing the centrifugal force against buoyancy and viscous drag. The density and viscosity increase at the gradient boundaries and should slow down the small graphene sheets while allowing larger and heavier sheets to pass through to the succeeding layers. When the centrifugal force is removed, CMG sheets with different lateral size and surface chemistry can thus be captured along the centrifuge tube at appropriate positions, as shown in Figure 1a. Digital camera images of the centrifugation tubes after separation under different conditions are shown in Figure 1b. The horizontal dark bands/lines correspond to the gradient boundaries as set before centrifugation, where CMG sheets of specific size and property accumulated.

Our first separation attempt was carried out using chemically reduced graphene oxide (CRG) sheets prepared by reduction of GO with hydrazine.[30] The as-prepared CRG have not been completely reduced, are still rich in surface functional groups,[31] and are thus dispersible in water and the aqueous gradient-making medium (sucrose solution) without agglomeration or requiring the presence of a surfactant;[30] this is the precondition for using the DGUR method. After the as-prepared CRG suspension was layered on top of the density gradient (20−66% gradient) (Figure 1b, tube A) and centrifuged at 50K rpm for 15 min, CRG sheets were separated into different zones along the centrifuge tube (Figure 1b, tube B). AFM characterization indicated that sampling along the centrifuge tube yielded CRG sheets of increasing size from 50 to 600 nm (Figure 2 and Figure S1 in the Supporting Information). AFM images of the GO and the unseparated CRG are shown in Figure S2 in the Supporting Information for comparison. The tapping-mode heights of fractions (~0.7 nm) confirmed the single-layered structures in all fractions after separation (Figure S3 in the Supporting Information). The results show that we can obtain almost monodisperse CRG sheets (see Figure S1 in the Supporting Information), with relatively small differences in sheet diameter, using this method.

Further study revealed that this method can serve as a general process for separation of crude CMG into monodisperse fractions. We evidenced this by employing the DGUR separation method with the precursor of CRG, GO. Following the same procedure, different GO sheets were captured at different positions along the centrifuge tube (Figure 1b, tube C). The size of the GO sheets increased from 40 nm

(f5) to 450 nm (f30), as revealed by AFM (see Figure 3 and Figure S4 in the Supporting Information). Black aggregates were found at the bottom of tube C in Figure 1b. TEM images of these aggregates revealed multilayered structures (see Figure 3g). This demonstrates that the DGUR method can separate single layer from multilayer GO sheets[39] because the thick and heavy multilayered structures sediment faster than single layered ones, while single layered sheets become sorted merely according to size.

Another feature of GO separation is that the color of the section near the bottom of the tube is "dark gray", which is different from the upper "yellow-brown" parts (Figure 1b, tube C). In order to study the composition of the "dark gray" material, we reduced the centrifugation time from 15 to 5 min to extend the range of materials separated. Digital images of different fractions from the resulting tube D (labeled as f5−f30 in Figure 1b) showed different colors (the insets in Figure 4a, and Figure S5a in the Supporting Information). Absorption measurements in the UV−vis range gave a clear trend after normalizing the curves to the absorbance of the peak around 230 nm, which corresponds to a π-electron plasmon excitation of graphitic carbon.[46,47] GO sheets in upper fractions (*e.g.*, f5) had much lower absorbance in the visible range, 400−800 nm, while the visible absorbance of lower fractions increased significantly (Figure 4a). The ratio of absorbance intensity at 400 nm to that at 800 nm ($Abs_{400\ nm}/Abs_{800\ nm}$) also decreased markedly with increasing fraction number (Figure 4b). Indeed, the absorbance curve of f30 was almost flat in the visible region ($Abs_{400\ nm}/Abs_{800\ nm}$ = 1.4:1), similar to that observed for the "pristine" graphene made by intercalation and exfoliation without oxidation,[48] while the absorbance curve of f5 ramped down sharply from 400 to 800 nm ($Abs_{400\ nm}/Abs_{800\ nm}$ = 4.5:1), comparable to that observed for fully oxidized GO.[13] This implies that GO sheets were separated in terms of degree of oxidation, with less functionalized graphene sheets being distributed in higher fraction numbers. This was further confirmed by the red shift of the UV absorption peak from *ca.* 230 nm for f5 to 260 nm for f30 (Figure 4c); such a red shift has previously been reported when the degree of reduction of GO is increased.[49]

The evolution of functionalization through the fractions was further evidenced by C_{1s} X-ray photoelectron spectroscopy (XPS, Figure 4d, 4e) and photoluminescence analysis (Figure 4f). The XPS spectrum of f30 showed a much weaker C−O peak (at *ca.* 286.5 eV) than upper fractions like f10 or that reported for GO.[50,51] This corresponds to a reduced number of epoxide and hydroxyl functional groups in the former,[52,53] *i.e.*, a lower degree of oxidation. Differences in extent of chemical functionalization also induced significant differences in fluorescence properties. f5 was the only fraction showing strong photoluminescence in the visible range,

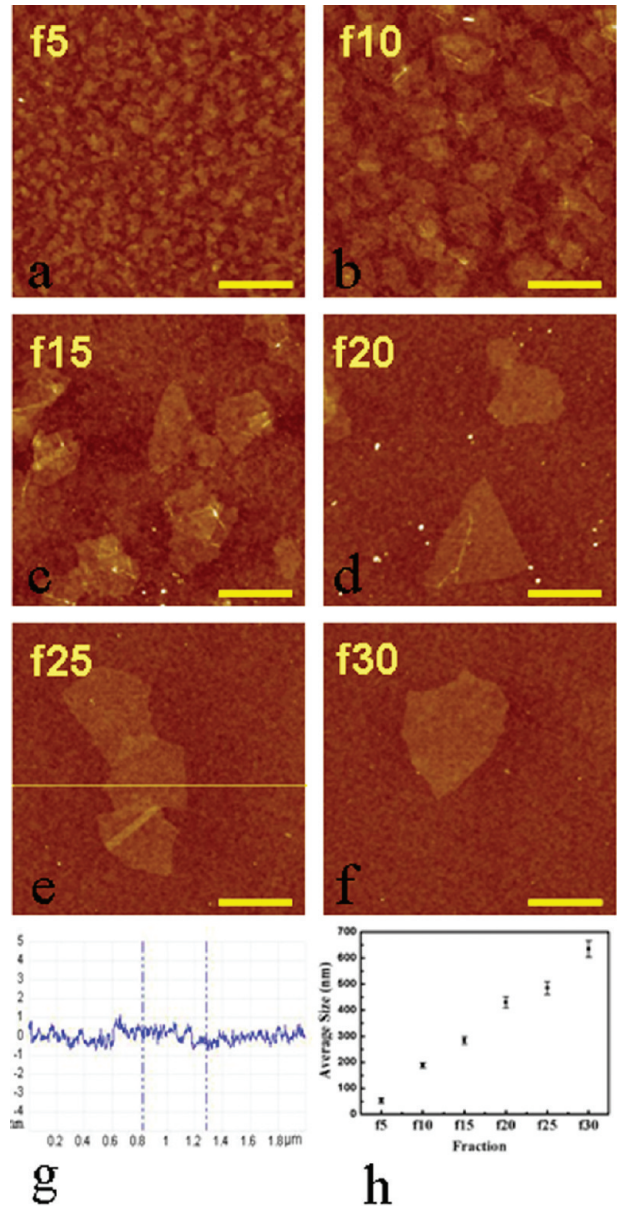

Figure 2. (a−f) Tapping-mode AFM images (2 × 2 μm², scale bar: 500 nm) of different fractions of CRG as labeled in tube B in Figure 1b. (g) Tapping-mode height images of CRG in fraction f25 from tube B in Figure 1b. (h) Variation in average size with fraction number.

which is consistent with the presence of GO sheets with extremely small size and a high degree of oxidation.[13] This fraction may be suitable for applications in cellular imaging and drug delivery.[13] The fluorescence intensity decreases in succeeding fractions and is negligible from f20 downward. The CMG sheets in these fractions might be more suitable for application in devices by virtue of their increased size (usually >400 nm) and low extent of oxidation (close to pristine graphene sheets).[5,48] Centrifugation for 5 min (tube D in Figure 1b) gives fractions separated in terms of oxidation degree and, for the more oxidized fractions (yellow-brown colored fractions) at least, an additional separation in terms of sheet size, as shown by the AFM results, which

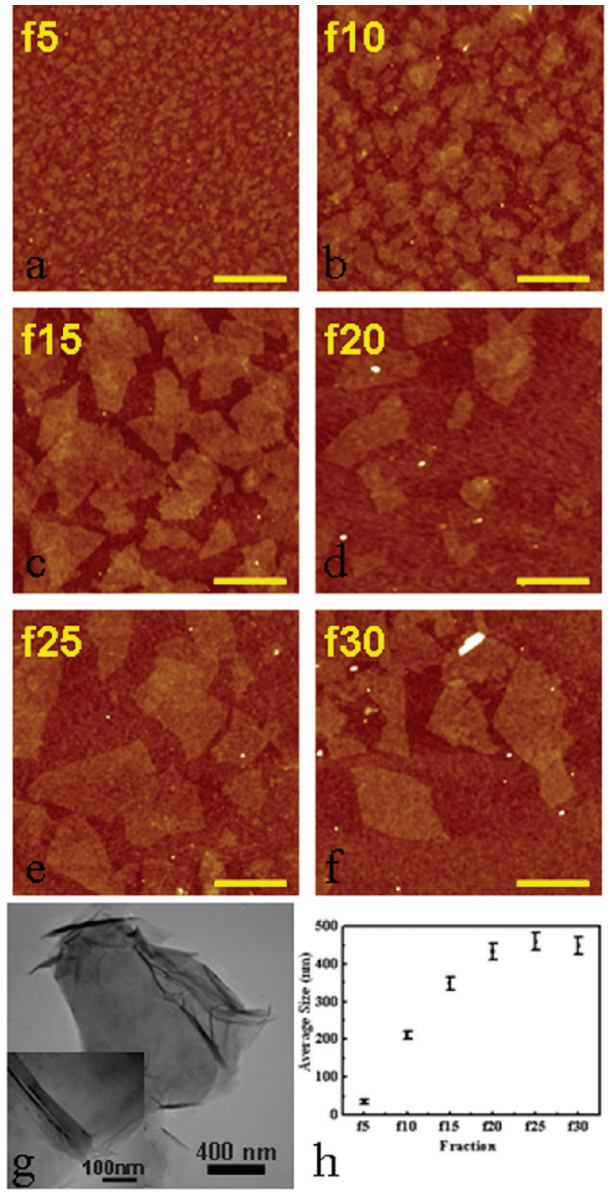

Figure 3. (a−f) Tapping-mode AFM images (2 × 2 μm², scale bar: 500 nm) of GO fractions separated in a 20−66% gradient for 15 min (fractions as labeled in tube C in Figure 1b. (g) TEM images of the black aggregates present at the bottom of the tube C in Figure 1b. (h) Variation in average size with fraction number.

reveal the size differences (Figures S6 and S7 in the Supporting Information). Somewhat unexpectedly, the Raman spectra of different GO fractions from f5 to f25 showed very little difference in the D- to G-band intensity ratio (Figure S5b in the Supporting Information). This shows that the intensity ratio of the D and G bands is not a reliable indicator of the degree of oxidation since it can be influenced by a number of other factors, including edges, charge puddles, ripples, and defects. Previous reports have also confirmed that reduction of GO does not necessarily result in a decrease in D/G intensity ratio.[25,51,54−57]

The above results also suggest that GO or CRG with a specific size range can be targeted by adjusting the parameters such as centrifuge time and density gradient profile. For instance, shortening the centrifugation time from 15 to 5 min leads to better separation of the black components with larger sheet sizes. Alternatively, if GO sheets with a lower extent of oxidation are the target product, a gradient with more concentrated layers (40%−66%) can be used to retain the more oxidized yellow-brown components at the very top positions but give higher resolution of the less oxidized dark-gray components by widening the spatial distribution (Figure 1b, tube E, and Figure S8 in the Supporting Information).

SEPARATION MECHANISM

What are the rules governing the separation of CMG in a gradient under ultracentrifugation? Why is a density gradient needed? Theoretical analysis and further experiments were carried out to answer these questions and hence reveal the principles underlying of the separation process.

According to the classical theory of colloids, the sedimentation rate of colloidal particles in a given medium with density ρ_m and viscosity η_m, in a centripetal force field of g', can be described as[43,45]

$$U = 2(\rho_p - \rho_m)(r + t)^2(g'/9\eta_m) \qquad (I)$$

Here r denotes the radius of the core material particle, t denotes the thickness of the solvation shell,[43] and ρ_p denotes the net density of the particle. Formula I indicates that the colloid sedimentation speed depends on both colloid core radius r (that is why large sheets sediment faster than small ones) and the properties of the medium (ρ_m and η_m). The density difference between ρ_p and ρ_m is the dominant term. The particles stop sedimentation when they reach a medium of the same density (*i.e.*, $\rho_p - \rho_m = 0$). This is how we estimate the net density of colloids by isopycnic separation.

In the case of CMG, the net density of the CMG sheets is highly dependent on both the sheet size and the hydration degree. A model of colloidal CMG is shown in Figure 5. In this model, it is assumed that (1) the CMG sheets are circular disks, with radius r, thickness h, and density ρ_c and (2) the CMG is surrounded by a disklike hydration shell, with thickness t and density 1 g/cm³.

Given the above assumptions, the net density of the CMG is given by formula II:

$$\rho_p = 1 + (\rho_c - 1)/[(1 + t/r)^2(1 + 2t/h)] \qquad (II)$$

Formula II indicates how the density difference between colloidal CMGs allows separation: when the graphene sheets are large ($r \uparrow$) or multilayer ($h \uparrow$), the net density increases and promotes sedimentation. As the oxidation degree increases, it results in the hydration layer becoming thicker ($t \uparrow$) so that the net density of the CMG decreases, which results in the col-

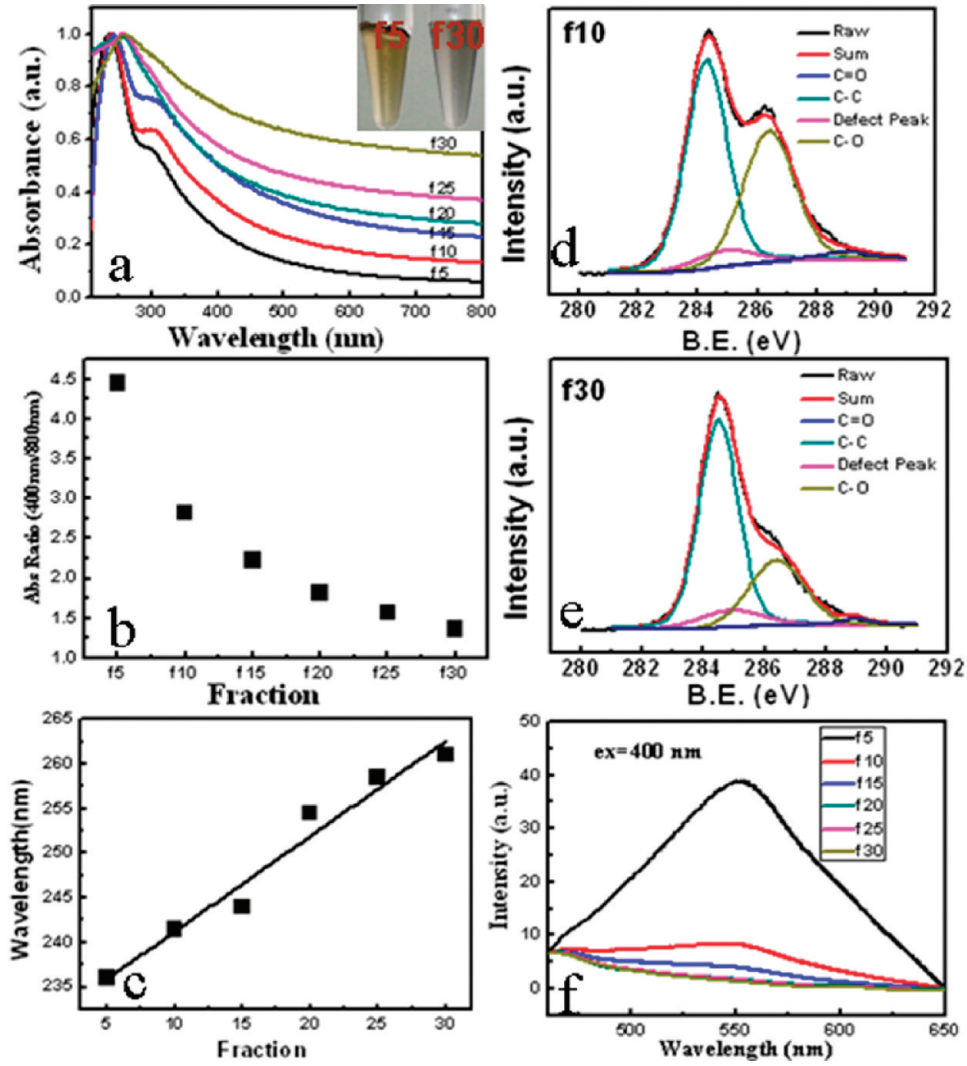

Figure 4. (a) UV−vis absorption spectra of GO in different fractions from tube D in Figure 1b. Inset: photograph of GO (f5 (left) and f30 (right)) after dilution. (b) Ratio of absorption at 400 nm to that at 800 nm of GO in different fractions from tube D in Figure 1b. (c) Variation in the wavelength of the absorption maximum of GO in different fractions from tube D in Figure 1b. (d, e) XPS spectra of f10 and f30 GO fractions from tube D in Figure 1b. (f) Fluorescence (λ_{ex} = 400 nm) spectra of GO in different fractions from tube D in Figure 1b.

loids being retained in the upper gradient layers. This explains why CMG can be separated under centrifugation according to differences in both the size of the sheets and the extent of oxidation.

To clarify the differences between GO and chemically reduced graphene oxide (CRG) sheets, isopycnic separations were performed in a linear density gradient (20−60%) at 32K rpm. In contrast to the short times (no more than 15 min) used in the above rate separations, the centrifugation time was extended to 12, 24, 36, and 48 h (see the digital images in Figure 6a and Figure S9 in the Supporting Information). Continual movements of CRG bands along the centrifuge tube indicated that the CRG sheets never became balanced with the buoyancy of the medium and finally aggregated at the bottom of the centrifugal tube, which implies their relative density is independent of size, confirming that isopycnic separation is ineffective. However, the movement of GO became significantly slower with increasing centrifugation time (Figure 6a). The sedimentation speed in the last 12 h was less than 2% of that in the first 15 min according to measurements on the yellow-brown section. During the last 12 h, the density gradient profile did not change significantly (Figure 6e). This implies that the GO sheet density was very close to

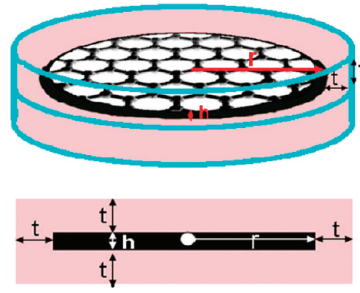

Figure 5. Illustrations of the hydrated colloidal CMG used in the model. Upper image: side view. Lower image: view along the direction perpendicular to the *c*-axis of the CMG sheets.

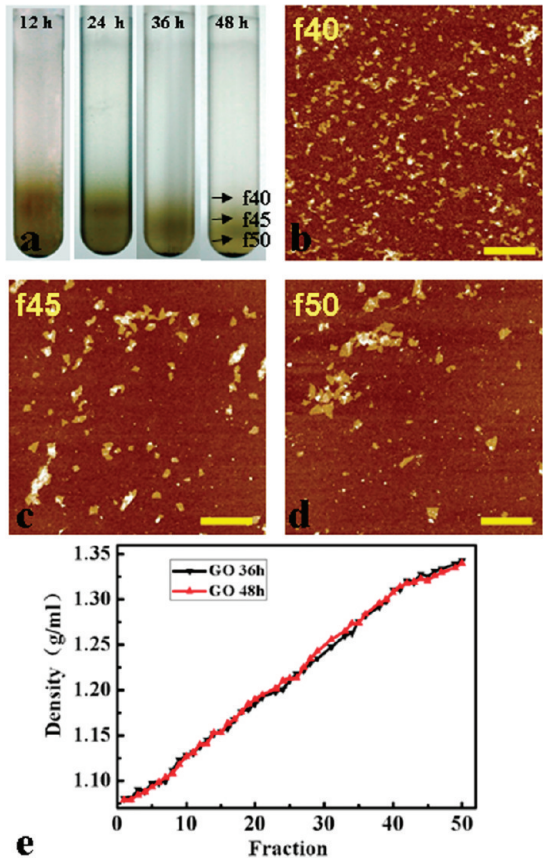

Figure 6. (a) Digital camera images of the ultracentrifuge tubes after separation at 32K rpm with different centrifuge times. (b-d) Tapping-mode AFM images (2 × 2 μm², scale bar: 400 nm) of GO fractions separated in a 20−60% linear gradient for 46 h. (e) Density curve of different fractions.

the ambient medium density (1.32 g/cm³) after centrifugation for 48 h. As revealed by AFM, the GO sheets still suspended in the sucrose medium (~60 wt %) were usually less than 200 nm in size (Figure 6b−d), while larger sheets have higher density and aggregated at the bottom of the centrifuge tube. It is reasonable to assume that GO sheets synthesized by Hummer's method have different degrees of oxidation because the graphitic carbon atoms at the edges and centers of the graphite particles have different chemical accessibility. Those located at the edges are more prone to higher degrees of oxidation. Smaller sheets have larger edge-to-area ratios and thus become more highly functionalized than larger sheets and therefore have a lower average density degree (see formula II above). The presence of the large number of functional groups located at the edges of graphene sheets also helps to stabilize colloidal GO suspension of smaller sheets. Larger sheets are less highly functionalized and retain higher densities, which explains why they were aggregated at the bottom of the centrifuge tube.

To answer the second question "Why is a density gradient necessary?", we used 30% sucrose as a uniform medium to separate CRG with the other conditions the same as those given in Figure 2 (same overall medium length, centrifugation at 50k rpm for 15 min). Digital photos and AFM images are shown in Figure 7. Some separation by size was obtained (Figures 7a to 7f), but some very small sheets accumulated in the top section (shown as a dark black band at the water/30% sucrose solution interface in Figure 7g). Furthermore, the sheet size near the bottom of the centrifuge tube was still small (<300 nm). This means the CRG size separation range shrunk from 50−700 nm for the density gradient method to 50−300 nm (a quantitative comparison of the two methods is shown in Figure 7h). The difference in separation ability of the two media is shown schematically in Figure 8. It can be seen that the multilayer gradients offer a combination of high resolution, narrow spatial distribution, and wide size range, while a single layer column only gives relatively high resolution over a smaller size range. Furthermore,

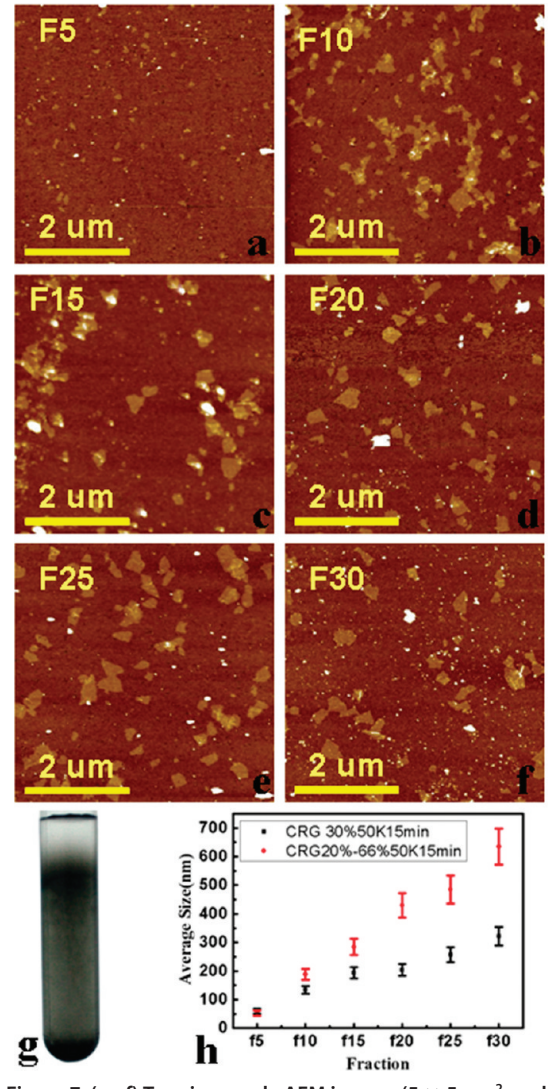

Figure 7. (a−f) Tapping-mode AFM images (5 × 5 μm², scale bar: 2 μm) of CRG fractions separated in 30% sucrose for 15 min. (g) Digital camera images of the ultracentrifuge tubes after separation. (h) Comparison of the average size in the fractions obtained using a density gradient (in red) and a uniform medium (in black), with the other separation conditions identical.

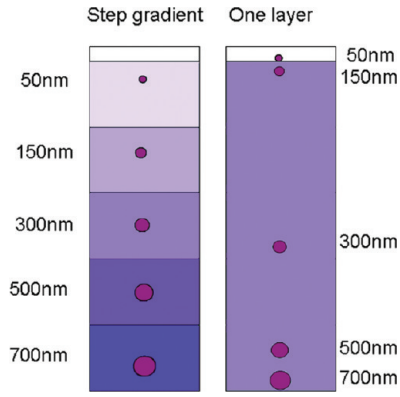

Figure 8. Comparison of separation effects with a density step gradient and one uniform layer.

even for the well-separated section, the colloids are significantly more diluted than for the multilayer gradient case. The wide size range and high spatial resolution obtained with the multilayer gradient separation are especially important when the method is employed for analysis of an unknown sample without any information available about choice of layer concentrations.

CONCLUSIONS

A density gradient ultracentrifugation rate separation method has been developed for sorting chemically modified graphenes by taking advantage of their differences in sedimentation rate. This rapid, versatile, scalable, efficient, nondestructive, and reproducible method separates single-layer and monodisperse GO and CRG sheets (50−700 nm) according to differences in size and chemical properties in a time as short as 5 min. Specific sheet size and extent of graphene functionalization can be targeted by adjusting the separation parameters, including centrifugation time and density gradient profile. Unwanted aggregates and even impurities (*e.g.*, silicates in graphene) were removed without interfering with the separation. The separation method provides a way of obtaining graphene sheets with suitable sizes in bulk quantities and might pave the way for realization of technological applications of graphene. It also provides a potential analytical method to assess the size distribution and stability of suspensions of CMG by comparison against standards.

EXPERIMENTAL SECTION

Preparation of Chemically Modified Graphene. Natural graphite materials were obtained from Pingdu Huadong Graphite Processing Factory (50 mesh, 99.95% purity). All other chemicals were A. R. grade, bought from Beijing Chemical Reagent Co., Inc., and used as received without further purification. Graphene oxide (GO) prepared by a modified Hummers method[3,30,58] was sonicated in water for 1 h to form an aqueous suspension (~1 mg/mL). The as-obtained GO materials were used for separation without any pretreatment.

DGUR Separation. We chose sucrose solutions with a suitable density distribution to prepare the density gradient, since sucrose gives solutions of appropriate viscosity and is low cost and environmentally friendly. In a typical procedure, 20%−66% (w/v) sucrose solutions were made with water. A step gradient was created directly in Beckman centrifuge tubes (polycarbonate, inner diameter 11 mm, length 60 mm) by adding layers (0.5 mL each) with increasing density (*i.e.*, increasing sucrose concentration) to the bottom of the tube. A freshly prepared GO suspension (0.2 mL) was immediately layered on top of the multilayer water−sucrose solution density gradient prior to ultracentrifugation. The typical centrifugation conditions were 5 min at 50K rpm (~300 kg, SW65 Rotor, Beckman Coulter). Calibrated micropipettors were used to manually sample 100 μL fractions along the centrifuge tube after ultracentrifugation. Different gradients were used to optimize the separation. For instance, steeper gradients with higher density were used for separation of larger and heavier samples.

Characterization. AFM (Multimode Nanoscope IIIa, Veeco Instruments) was used to determine GO sheet size and thickness. A silicon substrate was cleaned with acetone, methanol, and 2-propanol and then soaked in an aqueous solution of 3-aminopropyltriethoxysilane (APTES; 12 μL of APTES in 20 mL of H_2O) for 15 min. After being thoroughly rinsed with deionized H_2O and blow-dried with Ar, the substrate was then soaked in a solution of GO for 10 min. All samples were calcined at 350 °C to remove organic components before AFM observation. The morphology of multilayered GO was investigated by using a Hitachi H-800 transmission electron microscope (TEM) with an accelerating voltage of 200 kV. The optical properties of GO were characterized by UV−vis absorbance spectroscopy (UV-2501PC, Shimadzu, working in the 200−900 nm range) and fluorescence spectrometry (RF-5301PC, Shimadzu, λ_{ex} = 400 nm) at room temperature. Raman spectra were recorded from 800 to 3600 cm^{-1} on a Renishaw 1000 Confocal Raman Microprobe (Renishaw Instruments) using a 514 nm argon ion laser. XPS measurements were performed using an ESCALAB 250 instrument (Thermo Electron) with Al Kα radiation.

Acknowledgment. This work was supported by NSFC, the 973 Program (2009CB939802), the "111" Project (B07004), the Foundation for Authors of National Excellent Doctoral Dissertations of P. R. China, and the Program for New Century Excellent Talents in University.

Supporting Information Available: Experimental details, AFM images, and digital images are shown in the Supporting Information. This material is available free of charge *via* the Internet at http://pubs.acs.org.

REFERENCES AND NOTES

1. Geim, A. K.; Novoselov, K. S. The Rise of Graphene. *Nat. Mater.* **2007**, *6*, 183–191.
2. Li, X.; Wang, X.; Zhang, L.; Lee, S.; Dai, H. Chemically Derived, Ultrasmooth Graphene Nanoribbon Semiconductors. *Science* **2008**, *319*, 1229–1232.
3. Stankovich, S.; Dikin, D. A.; Dommett, G. H. B.; Kohlhaas, K. M.; Zimney, E. J.; Stach, E. A.; Piner, R. D.; Nguyen, S. T.; Ruoff, R. S. Graphene-Based Composite Materials. *Nature* **2006**, *442*, 282–286.
4. Dikin, D. A.; Stankovich, S.; Zimney, E. J.; Piner, R. D.; Dommett, G. H. B.; Evmenenko, G.; Nguyen, S. T.; Ruoff, R. S. Preparation and Characterization of Graphene Oxide Paper. *Nature* **2007**, *448*, 457–460.
5. Eda, G.; Fanchini, G.; Chhowalla, M. Large-Area Ultrathin Films of Reduced Graphene Oxide as A Transparent and Flexible Electronic Material. *Nat. Nanotechnol.* **2008**, *3*, 270–274.
6. Fowler, J. D.; Allen, M. J.; Tung, V. C.; Yang, Y.; Kaner, R. B.; Weiller, B. H. Practical Chemical Sensors from Chemically Derived Graphene. *ACS Nano* **2009**, *3*, 301–306.
7. Wang, L.; Lee, K.; Sun, Y.-Y.; Lucking, M.; Chen, Z.; Zhao, J. J.; Zhang, S. B. Graphene Oxide as an Ideal Substrate for Hydrogen Storage. *ACS Nano* **2009**, *3*, 2995–3000.

8. Bunch, J. S.; van der Zande, A. M.; Verbridge, S. S.; Frank, I. W.; Tanenbaum, D. M.; Parpia, J. M.; Craighead, H. G.; McEuen, P. L. Electromechanical Resonators from Graphene Sheets. *Science* **2007**, *315*, 490–493.
9. Kopelevich, Y.; Esquinazi, P. Graphene Physics in Graphite. *Adv. Mater.* **2007**, *19*, 4559–4563.
10. Novoselov, K. S.; Geim, A. K.; Morozov, S. V.; Jiang, D.; Katsnelson, M. I.; Grigorieva, I. V.; Dubonos, S. V.; Firsov, A. A. Two-Dimensional Gas of Massless Dirac Fermions in Graphene. *Nature* **2005**, *438*, 197–200.
11. Yin, Z.; Wu, S.; Zhou, X.; Huang, X.; Zhang, Q.; Boey, F.; Zhang, H. Electrochemical Deposition of ZnO Nanorods on Transparent Reduced Graphene Oxide Electrodes for Hybrid Solar Cells. *Small* **2010**, *6*, 307–312.
12. Ang, P. K.; Wang, S.; Bao, Q.; Thong, J. T. L.; Loh, K. P. High-Throughput Synthesis of Graphene by Intercalation-Exfoliation of Graphite Oxide and Study of Ionic Screening in Graphene Transistor. *ACS Nano* **2009**, *3*, 3587–3594.
13. Sun, X.; Liu, Z.; Welsher, K.; Robinson, J. T.; Goodwin, A.; Zaric, S.; Dai, H. Nano-Graphene Oxide for Cellular Imaging and Drug Delivery. *Nano Res.* **2008**, *1*, 203–212.
14. Liu, Z.; Robinson, J. T.; Sun, X.; Dai, H. PEGylated Nanographene Oxide for Delivery of Water-Insoluble Cancer Drugs. *J. Am. Chem. Soc.* **2008**, *130*, 10876–10877.
15. Agarwal, S.-C.; Zhou, X.-Z.; Ye, F.; He, Q.-Y.; Chen, G. C. K.; Soo, J.-C.; Boey, F.; Zhang, H.; Chen, P. Interfacing Live Cells with Nanocarbon Substrates. *Langmuir* **2010**, *26*, 2244–2247.
16. Mattevi, C.; Eda, G.; Agnoli, S.; Miller, S.; Mkhoyan, K. A.; Celik, O.; Mastrogiovanni, D.; Granozzi, G.; Garfunkel, E.; Chhowalla, M. Evolution of Electrical, Chemical, and Structural Properties of Transparent and Conducting Chemically Derived Graphene Thin Films. *Adv. Funct. Mater.* **2009**, *19*, 2577–2583.
17. Tang, L.; Wang, Y.; Li, Y.; Feng, H.; Lu, J.; Li, J. Preparation, Structure, and Electrochemical Properties of Reduced Graphene Sheet Films. *Adv. Funct. Mater.* **2009**, *19*, 2782–2789.
18. Becerril, H. A.; Mao, J.; Liu, Z.; Stoltenberg, R. M.; Bao, Z.; Chen, Y. Evaluation of Solution-Processed Reduced Graphene Oxide Films as Transparent Conductors. *ACS Nano* **2008**, 463–470.
19. Wang, S.; Ang, P. K.; Wang, Z.; Tang, A. L. L.; Thong, J. T. L.; Loh, K. P. High Mobility, Printable, and Solution-Processed Graphene Electronics. *Nano Lett.* **2010**, *10*, 92–98.
20. Lomeda, J. R.; Doyle, C. D.; Kosynkin, D. V.; Hwang, W.-F.; Tour, J. M. Diazonium Functionalization of Surfactant-Wrapped Chemically Converted Graphene Sheets. *J. Am. Chem. Soc.* **2008**, *130*, 16201–16206.
21. Park, S.; Ruoff, R. S. Chemical Methods for the Production of Graphenes. *Nat. Nanotechnol.* **2009**, *4*, 217–224.
22. Liu, N.; Luo, F.; Wu, H.; Liu, Y.; Zhang, C.; Chen, J. One-step Ionic-Liquid-Assisted Electrochemical Synthesis of Ionic-Liquid-Functionalized Graphene Sheets Directly from Graphite. *Adv. Funct. Mater.* **2008**, *18*, 1518–1525.
23. Park, S.; An, J.; Jung, I.; Piner, R. D.; An, S. J.; Li, X.; Velamakanni, A.; Ruoff, R. S. Colloidal Suspensions of Highly Reduced Graphene Oxide in a Wide Variety of Organic Solvents. *Nano Lett.* **2009**, *9*, 1593–1597.
24. Tung, V. C.; Allen, M. J.; Yang, Y.; Kaner, R. B. High-Throughput Solution Processing of Large-Scale Graphene. *Nat. Nanotechnol.* **2008**, *4*, 25–29.
25. Stankovich, S.; Dikin, D. A.; Piner, R. D.; Kohlhaas, K. A.; Kleinhammes, A.; Jia, Y.; Wu, Y.; Nguyen, S. T.; Ruoff, R. S. Synthesis of Graphene-Based Nanosheets *via* Chemical Reduction of Exfoliated Graphite Oxide. *Carbon* **2007**, *45*, 1558–1565.
26. Liang, Y.; Wu, D.; Feng, X.; Muellen, K. Dispersion of Graphene Sheets in Organic Solvent Supported by Ionic Interactions. *Adv. Mater.* **2009**, *21*, 1679–1683.
27. Wang, Z.; Zhou, X.; Zhang, J.; Boey, F.; Zhang, H. Direct Electrochemical Reduction of Single-Layer Graphene Oxide and Subsequent Functionalization with Glucose Oxidase. *J. Phys. Chem. C* **2009**, *113*, 14071–14075.
28. Zhou, X.; Huang, X.; Qi, X.; Wu, S.; Xue, C.; Boey, F. Y. C.; Yan, Q.; Chen, P.; Zhang, H. In Situ Synthesis of Metal Nanoparticles on Single-Layer Graphene Oxide and Reduced Graphene Oxide Surfaces. *J. Phys. Chem. C* **2009**, *113*, 10842–10846.
29. Huang, X.; Zhou, X.; Wu, S.; Wei, Y.; Qi, X.; Zhang, J.; Boey, F.; Zhang, H. Reduced Graphene Oxide-Templated Photochemical Synthesis and in situ Assembly of Au Nanodots to Orderly Patterned Au Nanodot Chains. *Small* **2010**, *6*, 513–516.
30. Li, D.; Mueller, M. B.; Gilje, S.; Kaner, R. B.; Wallace, G. G. Processable Aqueous Dispersions of Graphene Nanosheets. *Nat. Nanotechnol.* **2008**, *3*, 101–105.
31. Li, D.; Kaner, R. B. Graphene-Based Materials. *Science* **2008**, *320*, 1170–1171.
32. Wang, X.; Peng, Q.; Li, Y. Interface-Mediated Growth of Monodispersed Nanostructures. *Acc. Chem. Res.* **2007**, *40*, 635–643.
33. Jun, Y.-w.; Choi, J.-s.; Cheon, J. Shape Control of Semiconductor and Metal Oxide Nanocrystals through Nonhydrolytic Colloidal Routes. *Angew. Chem., Int. Ed.* **2006**, *45*, 3414–3439.
34. Arnold, M. S.; Stupp, S. I.; Hersam, M. C. Enrichment of Single-Walled Carbon Nanotubes by Diameter in Density Gradients. *Nano Lett.* **2005**, *5*, 713–718.
35. Green, A. A.; Hersam, M. C. Processing and Properties of Highly Enriched Double-Wall Carbon Nanotubes. *Nat. Nanotechnol.* **2009**, *4*, 64–70.
36. Arnold, M. S.; Green, A. A.; Hulvat, J. F.; Stupp, S. I.; Hersam, M. C. Sorting Carbon Nanotubes by Electronic Structure using Density Differentiation. *Nat. Nanotechnol.* **2006**, *1*, 60–65.
37. Wei, L.; Lee, C. W.; Li, L.-J.; Sudibya, H. G.; Wang, B.; Chen, L. Q.; Chen, P.; Yang, Y.; Chan-Park, M. B.; Chen, Y. Assessment of (n,m) Selectively Enriched Small Diameter Single-Walled Carbon Nanotubes by Density Differentiation from Cobalt-Incorporated MCM-41 for Macroelectronics. *Chem. Mater.* **2008**, *20*, 7417–7424.
38. Haroz, E. H.; Rice, W. D.; Lu, B. Y.; Ghosh, S.; Hauge, R. H.; Weisman, R. B.; Doorn, S. K.; Kono, J. Enrichment of Armchair Carbon Nanotubes *via* Density Gradient Ultracentrifugation: Raman Spectroscopy Evidence. *ACS Nano* **2010**, *4*, 1955–1962.
39. Green, A. A.; Hersam, M. C. Solution Phase Production of Graphene with Controlled Thickness *via* Density Differentiation. *Nano Lett.* **2009**, *9*, 4031–4036.
40. Green, A. A.; Hersam, M. C. Emerging Methods for Producing Monodisperse Graphene Dispersions. *J. Phys. Chem. Lett.* **2010**, *1*, 544–549.
41. Sun, X.; Zaric, S.; Daranciang, D.; Welsher, K.; Lu, Y.; Li, X.; Dai, H. Optical Properties of Ultrashort Semiconducting Single-Walled Carbon Nanotube Capsules Down to Sub-10 nm. *J. Am. Chem. Soc.* **2008**, *130*, 6551–6555.
42. Fagan, J. A.; Becker, M. L.; Chun, J.; Hobbie, E. K. Length Fractionation of Carbon Nanotubes Using Centrifugation. *Adv. Mater.* **2008**, *20*, 1609–1613.
43. Sun, X.; Tabakman, S. M.; Seo, W.-S.; Zhang, L.; Zhang, G.; Sherlock, S.; Bai, L.; Dai, H. Separation of Nanoparticles in a Density Gradient: FeCo@C and Gold Nanocrystals. *Angew. Chem., Int. Ed.* **2009**, *48*, 939–942.
44. Brakke, M. K. Density Gradient Centrifugation: A New Separation Technique. *J. Am. Chem. Soc.* **1951**, *73*, 1847–1848.
45. Price, C. A. *Centrifugation in Density Gradients*; Academic Press: New York, 1982.
46. Reed, B. W.; Sarikaya, M. Electronic Properties of Carbon Nanotubes by Transmission Electron Energy-Loss Spectroscopy. *Phy. Rev. B* **2001**, *64*, 195404/1–195404/13.
47. Attal, S.; Thiruvengadathan, R.; Regev, O. Determination of the Concentration of Single-Walled Carbon Nanotubes in Aqueous Dispersions Using UV−Visible Absorption Spectroscopy. *Anal. Chem.* **2006**, *78*, 8098–8104.
48. Li, X.; Zhang, G.; Bai, X.; Sun, X.; Wang, X.; Wang, E.; Dai, H. Highly Conducting Graphene Sheets and Langmuir−Blodgett Films. *Nat. Nanotechnol.* **2008**, *3*, 538–542.

49. Wang, W. L.; Meng, S.; Kaxiras, E. Graphene NanoFlakes with Large Spin. *Nano Lett.* **2008**, *8*, 241–245.
50. Yang, D.; Velamakanni, A.; Bozoklu, G.; Park, S.; Stoller, M.; Piner, R. D.; Stankovich, S.; Jung, I.; Field, D. A.; Ventrice, C. A., Jr.; Ruoff, R. S. Chemical Analysis of Graphene Oxide Films after Heat and Chemical Treatments by X-Ray Photoelectron and Micro-Raman Spectroscopy. *Carbon* **2009**, *47*, 145–152.
51. Akhavan, O. The Effect of Heat Treatment on Formation of Graphene Thin Films from Graphene Oxide Nanosheets. *Carbon* **2009**, *48*, 509–519.
52. Fan, X.; Peng, W.; Li, Y.; Li, X.; Wang, S.; Zhang, G.; Zhang, F. Deoxygenation of Exfoliated Graphite Oxide under Alkaline Conditions: A Green Route to Graphene Preparation. *Adv. Mater.* **2008**, *20*, 4490–4493.
53. Zhou, Y.; Bao, Q.; Tang, L. A. L.; Zhong, Y.; Loh, K. P. Hydrothermal Dehydration for the "Green" Reduction of Exfoliated Graphene Oxide to Graphene and Demonstration of Tunable Optical Limiting Properties. *Chem. Mater.* **2009**, *21*, 2950–2956.
54. Rao, C. N. R.; Sood, A. K.; Subrahmanyam, K. S.; Govindaraj, A. Graphene: The New Two-Dimensional Nanomaterial. *Angew. Chem., Int. Ed.* **2009**, *48*, 7752–7777.
55. Ferrari, A. C. Raman Spectroscopy of Graphene and Graphite: Disorder, Electron-Phonon Coupling, Doping and Nonadiabatic Effects. *Solid State Commun.* **2007**, *143*, 47–57.
56. Gomez-Navarro, C.; Weitz, R. T.; Bittner, A. M.; Scolari, M.; Mews, A.; Burghard, M.; Kern, K. Electronic Transport Properties of Individual Chemically Reduced Graphene Oxide Sheets. *Nano Lett.* **2007**, *7*, 3499–3503.
57. Wang, H.; Robinson, J. T.; Li, X.; Dai, H. Solvothermal Reduction of Chemically Exfoliated Graphene Sheets. *J. Am. Chem. Soc.* **2009**, *131*, 9910–9911.
58. Hummers, W. S.; Offeman, R. E. Preparation of Graphitic Oxide. *J. Am. Chem. Soc.* **1958**, *80*, 1339.